PREPARATION OF Fe_3O_4-ZnO-CuO NANOCOMPOSITES WITH DIFFERENT MOLE RATIOS AND THEIR CHARACTERIZATIONS

Ei Ei Phyo Cin[1] , Khin Mar Cho[2], Yee Mun Than[3]

Abstract

Magnetically separable Fe_3O_4-ZnO-CuO nanocomposites were prepared by sol-gel method. The XRD pattern of Fe_3O_4- ZnO- CuO nanocomposite showed the presence of Fe_3O_4, ZnO and CuO peaks. The crystallite sizes of Fe_3O_4- ZnO-0.5CuO, Fe_3O_4- ZnO- 1CuO, Fe_3O_4- ZnO- 2.5CuO and Fe_3O_4- ZnO- 5CuO nanocomposites were also calculated as 34.1 nm, 23.4 nm, 25.1 nm and 24.4 nm respectively. Characteristic peaks of Fe-O, Zn-O and Cu-O were found in the FT IR spectra. SEM images of Fe_3O_4- ZnO- CuO nanocomposite showed both spherical and clew like shaped particles. EDS showed the presence of Fe, Zn, Cu and O elements in Fe_3O_4- ZnO- CuO nanocomposite. Fe_3O_4- ZnO- CuO nanocomposites with different mole ratios were found to have cubic structure and TEM image of Fe_3O_4-ZnO-CuO nanocomposite also showed the cubic morphology. By TG-DTA weight loss less than 7 % were indicated thermal stability of the prepared of Fe_3O_4- ZnO- CuO nanocomposite.

Keywords: nanocomposite, sol-gel method, cubic morphology, thermal stability

Introduction

Nanomaterial is a material with the size of nanoscale (1-100 nm). This material has a unique properties and high value for commercial applications. The key factors of nanoparticles are small particle size, narrow size distribution, low agglomeration and high dispersion. Nanomaterial can be applied in various fields such as cosmetics, paints, displays, batteries, medicine, catalysis, gas sensor, food engineering (production, processing, safety and packaging), agriculture, energy (storage and conversion) and construction (Akir *et al*., 2016).

The semiconductor zinc oxide (ZnO) is one of the most efficient and environmentally-friendly catalysts because of its non-toxicity, low cost, good catalytic performance and high stability. However, ZnO having direct wide band-gap (~3.24 eV) is only responsive to ultraviolet (UV) light and reduces its efficiency in visible light. ZnO causes a high recombination rate of electron and hole which are produced due to the irradiation of light (Hou *et al*., 2015; Akir *et al*., 2016). Therefore, to overcome these limitations, methods like doping, coupled with another semiconductor and deposition of noble metal can be used for the modification of ZnO (Mageshwari *et al*., 2016). Combining ZnO with CuO helps in separating photogenerated electron-hole pairs, which is crucial for effective photocatalysis and thus, increasing the degradation efficiency of organic dye (Taufik and Saleh, 2017).

In general, after the completion of the photocatalytic reaction it is difficult to recover the photocatalyst from the mixture. Since Fe_3O_4 has not only the good adsorption capacity but also possesses magnetic property it can magnetically separate the catalyst from organic dye solution easier.

Thus, a magnetic material such as Fe_3O_4 coupled with the ZnO-CuO nanocomposite can be used for the removal of dye and to be reused the composite by magnetic isolation (Heravi *et al*., 2015). Magnetic separation is an easy and time saving method for separating and recycling materials used as photocatalysts under a suitable magnetic field. This method can reduce the extent of agglomeration during recovery and can improve the reusability of the catalyst (Xuan *et al*., 2008).

[1] Lecturer, Department of Chemistry, Taunggoke Degree College
[2] Associate Professor, Department of Chemistry, University of Yangon
[3] Lecturer, Department of Chemistry, University of Yangon

The main aim of this research is to synthesize the magnetically separable Fe_3O_4- ZnO- CuO nanocomposites with different mole ratios by sol-gel method and structurally characterize.

Materials and Methods

Preparation of CuO Nanoparticles

CuO nanoparticles were prepared by sol-gel method as described by Taufik *et al*., (2015) with some modifications.

Briefly, 150 mL of 0.33 M sodium hydroxide solution was added drop-wise into 100 mL of 0.25 M Cu $(NO_3)_2$. $3H_2O$ solution (0.25 mol) in a 500 mL beaker with constant stirring in one direction until pH 12 was reached. Then, it was kept at 80˚C under magnetically stirring for 3 h to from a gel. After drying the gel at 80˚C for 4 h, it was annealed at 125˚C for 5 h to get black powder of CuO. The gel was then annealed at 600˚C for 5 h in a muffle furnace.

In similar way, the procedure was carried out using 0.125 M, 0.625 M and 1.25 M of $Cu(NO_3)_2.3H_2O$ solutions were used to get different mole ratios of the nanocomposites.

Preparation of Fe_3O_4 Nanoparticles

Fe_3O_4 nanoparticles were prepared by sol-gel method as described by Taufik *et al*., (2015) with some modifications.

Firstly, 5 mL of glacial acetic acid (CH_3COOH) and 30 mL of ethylene glycol $(CH_2OH)_2$ were added into 100 mL of 0.25 M $FeSO_4.7H_2O$ solution(0.025 mol) in a 500 mL beaker while stirring continuously until pH value of 3 was reached. After that, 150 mL of 0.33 M of sodium hydroxide solution was added drop-wise into the above solution with constant stirring in one direction until pH 3 was reached. The final solution was kept at 80˚C under magnetically stirring for 3h to from a gel. After drying the gel at 80˚C for 4 h, it was annealed at 125˚C for 3 h to get black powder of Fe_3O_4.

Preparation of Different Mole Ratios of Fe_3O_4-ZnO-CuO Nanocomposite

Fe_3O_4-ZnO-CuO nanocomposite was prepared by sol-gel method as described by

Taufik *et al*., (2015) with some modifications.

Firstly, 50 mL of 0.5 M of NaOH solution (0.025 mol) was added drop-wise into 100 mL of 0.25 M $ZnSO_4.7H_2O$ solution (0.125 mol). This solution is designated as solution A and it was stirred and heated at 80˚C. Meanwhile, the above synthesized Fe_3O_4 and CuO nanoparticles were dispersed in 30 mL each of ethanol and were designated as solutions B and C, respectively. After that, solutions B and C were added into solution A and the mixtures were continuously stirred at 80˚C for 2 h. Then, the mixtures were centrifuged and washed for several times with ethanol and distilled water. The final product was allowed to stand overnight at room temperature and then heated at 125˚C for 5 h under vacuum condition. In this way Fe_3O_4- ZnO-CuO nanocomposite was obtained. The following mole ratios of metal oxides were used as described in Table 1 to get other mole ratios of nanocomposites.

Table 1 Mole Ratios of Metal Oxides for Fe_3O_4-ZnO-CuO Nanocomposites

No	Sample	Mole of Metal Oxide (mol)		
		ZnO	Fe_3O_4	CuO
1	Fe_3O_4-ZnO-0.5 CuO	0.025	0.025	0.0125
2	Fe_3O_4-ZnO-1.0 CuO	0.025	0.025	0.0250
3	Fe_3O_4-ZnO-2.5 CuO	0.025	0.025	0.0625
4	Fe_3O_4-ZnO-5.0 CuO	0.025	0.025	0.1250

Characterization Techniques

The phase purity was examined by using Rigaku X-ray diffractometer (Rigaku Co., Japan) with Cu K_α (λ=1.54056 Å) radiation over a range of 2θ angles from 10˚ to 70˚. The average crystallite size was also calculated using the data obtained from diffractogram by Scherer's formula. Fourier transform infrared (FT IR) spectra of the samples were recorded on a FT IR spectrometer (FT IR-8400 SHIMADZU, Japan) in a range of wavenumber from 4000 to 500 cm^{-1}. Surface morphology of each of the prepared samples was studied by scanning electron microscope and energy dispersive X- ray spectroscopy (SEM-EDS) (Phenom PROX, Netherlands) Pyin Oo Lwin. Samples were also investigated by transmission electron microscope (TEM, JEOL TEM-3010 with an accelerating voltage of 100 kV at State Key Laboratory, College of Science, Beijing University of Chemical Technology, China. Thermo gravimetric - Differential Analysis (TG-DTA) was performed at Universities' Research Center, Yangon. TG-DTA thermogram was obtained by using Al_2O_3 as reference. The measurements were carried out at a heating rate of 20.0kJ $min^{-1}$and scanning from 40˚C to 600˚C with a scanning rate of 20˚C min^{-1}, under nitrogen atmosphere of 20 psi.

Results and Discussion

Characterization by X-Ray Diffraction Analysis

The phase purity, crystallite sizes and crystal structures of Fe_3O_4, CuO and Fe_3O_4- ZnO- CuO nanocomposite were investigated by X-ray diffraction analysis. Figure 1(a) shows the X-ray diffraction pattern of Fe_3O_4 nanoparticles. All the peaks of the (111), (220), (311), (222), (400), (422), (511) and (440) in XRD pattern were well - matched with standard diffraction pattern of Fe_3O_4(88-0315 > Magnetite). Only single phase of $Fe_3O_4$with no other phase was found in this XRD pattern. It indicates the purity of the Fe_3O_4 sample. Figure 1(b) shows the X-ray diffraction pattern of CuO nanoparticles. Similarly, in the XRD pattern of CuO, all peaks were well - matched with standard diffraction pattern of CuO (85-5889 > CuO). No other impurity peaks were observed. The X-ray diffraction patterns of Fe_3O_4- ZnO- CuO nanocomposites with different mole ratios are depicted in Figures 2 (a), 2(b), 2(c) and 2(e). It was seen that additional peaks other than Fe_3O_4 peaks and CuO peaks appeared in the X-ray diffractogram due to the presence of ZnO NPs. In these diffractogram of the composites the Fe_3O_4 peaks and CuO peaks were observed to be slightly shifted from their peak positions. Furthermore, the diffractogram showed only Fe_3O_4, ZnO and CuO phases and it indicated the absence of impurities.

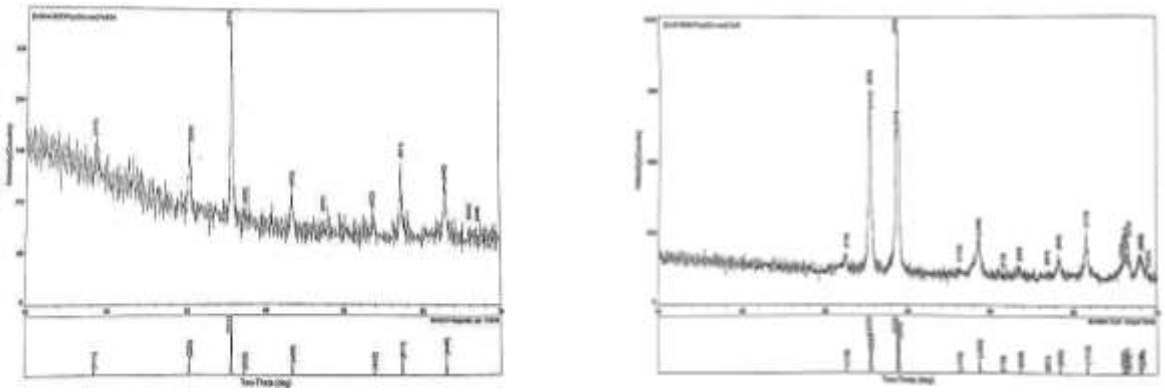

(a) (b)

Figure 1 X-ray diffraction patterns of (a) Fe_3O_4 and (b) CuO

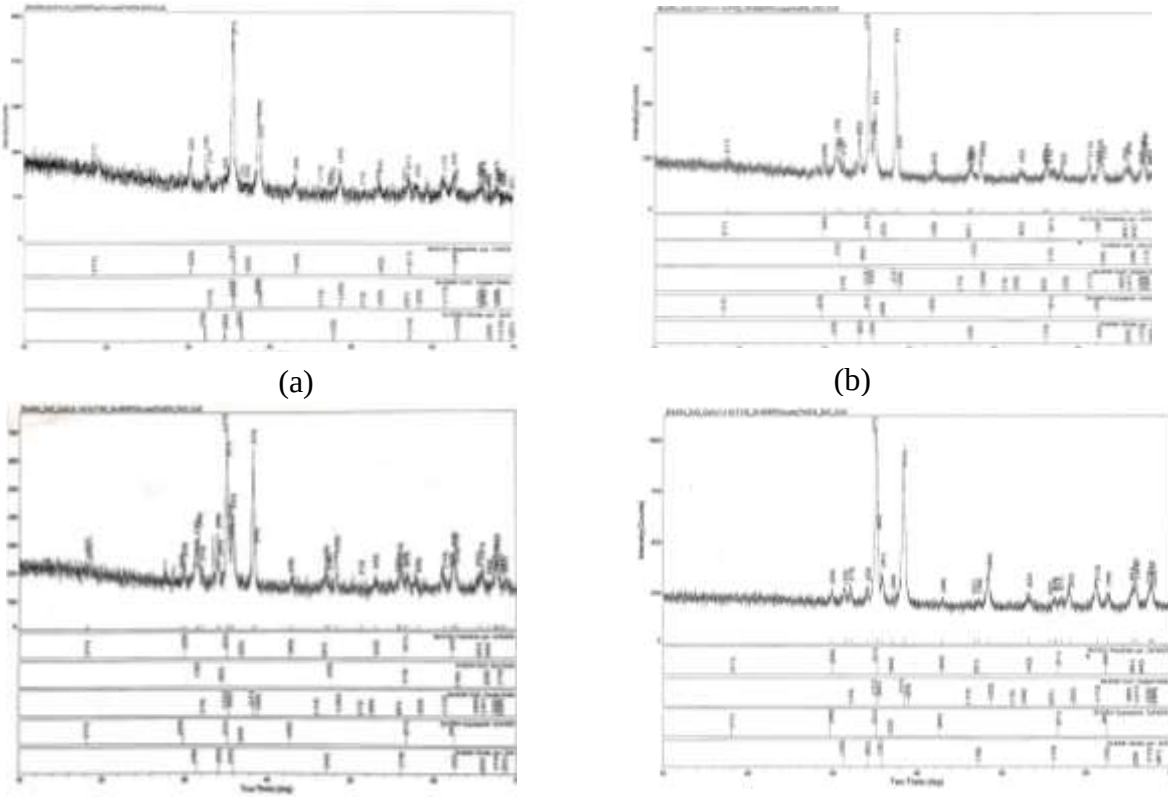

(a) (b)

(c) (d)

Figure 2 X-ray diffraction patterns of (a) Fe_3O_4- ZnO-0.5CuO (b) Fe_3O_4- ZnO-1 CuO (c) Fe_3O_4-ZnO-2.5 CuO (d) Fe_3O_4- ZnO-5CuO nanocomposites

The average crystallite sizes of samples were calculated from the dominant peaks of X-ray line broadening planes using Scherrer equation, $\tau = \frac{0.9\lambda}{\beta\cos\theta}$ in which τ is the crystallite size (nm), λ is the diffraction wavelength (0.154059 nm for Cu K_α radiation), θ is the diffraction angle (degree) and 'β' is the full width at half maximum (FWHM) for the diffraction peak (radian) . Table 2 shows the crystallite sizes of Fe_3O_4 nanoparticles, CuO nanoparticles and Fe_3O_4 -ZnO -CuO nanocomposites with different mole ratios. Crystallite sizes of Fe_3O_4-ZnO-CuO nanocomposites were larger than CuO nanoparticles (21.5 nm) and the crystallite sizes of the nanocomposites were not much different except Fe_3O_4 - ZnO - 0.5CuO nanocomposites which was 34.1 nm.

Table 3 shows the lattice constants of Fe_3O_4 nanoparticles, CuO nanoparticles and Fe_3O_4-ZnO-CuO nanocomposites. CuO was indexed as monoclinic with 'a' (4.6843 Å) and 'b' (3.4261 Å)· and longer 'c' (5.1254 Å) whereas Fe_3O_4 and the composites were cubic with equal lengths.

Table 2 Crystallite Sizes of Fe_3O_4 -ZnO -CuO Nanocomposites with Different Mole Ratios

No	Sample	Calculated Crystallite Size (nm)
1	Fe_3O_4 nanoparticles	29.6
2	CuO nanoparticles	21.5
3	Fe_3O_4 -ZnO - 0.5CuO nanocomposites	34.1
4	Fe_3O_4 -ZnO -1 CuO nanocomposites	23.4
5	Fe_3O_4 -ZnO - 2.5CuO nanocomposites	25.1
6	Fe_3O_4 -ZnO - 5CuO nanocomposites	24.4

Table 3 Lattice Constants of Fe_3O_4-ZnO-CuO Nanocomposites with Different Mole Ratios

No	Sample	Axial length (Å)			Interaxial angle(º)			Crystal structure
		a	b	c	α	β	γ	
1	Fe_3O_4	8.3482	8.3482	8.3482	90	90	90	Cubic
2	CuO	4.6843	3.4281	5.1254	90	99.27	90	Monoclinic
3	Fe_3O_4 –ZnO-0.5CuO	6.2226	6.2226	6.2225	90	90	90	Cubic
4	Fe_3O_4 -ZnO -1.0CuO	6.2167	6.2167	6.2167	90	90	90	Cubic
5	Fe_3O_4 –ZnO-2.5CuO	6.2480	6.2480	6.2480	90	90	90	Cubic
6	Fe_3O_4 –ZnO-5.0CuO	6.2361	6.2361	6.2361	90	90	90	Cubic

Characterization by FT IR

Figure 3 shows the FT IR spectra of Fe_3O_4-ZnO-CuO nanocomposites and interpretation of the spectral data are described in Table 4. Characteristic vibration peaks of Fe-O appeared between 570-580 cm^{-1}, Cu-O between 830-875 $cm^{-1}$and Zn-O peaks between 615-623 cm^{-1} in the Fe_3O_4-ZnO-CuO nanocomposites.

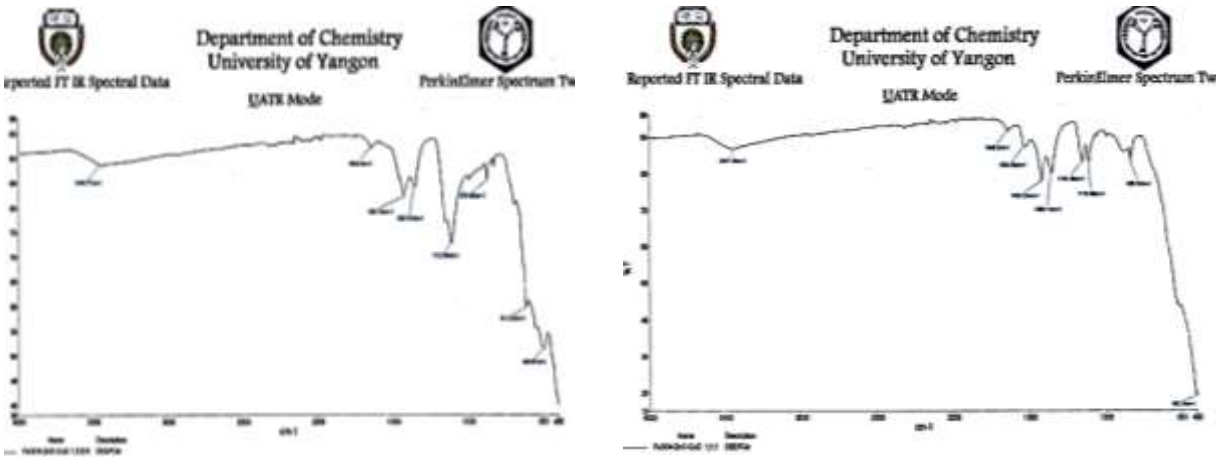

(a) (b)

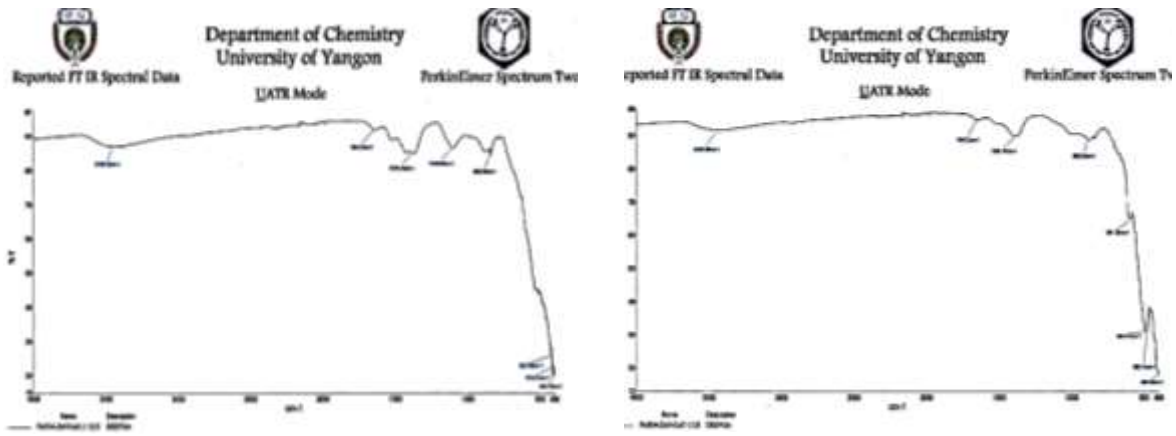

(c) (d)

Figure 3 FT-IR spectra of (a) Fe_3O_4- ZnO- 0.5CuO (b) Fe_3O_4- ZnO- CuO (c) Fe_3O_4- ZnO- 2.5CuO (d) Fe_3O_4-ZnO-5CuO nanocomposites

Table 4 FT IR Spectral Data of Fe_3O_4-ZnO-CuO Nanocomposites with Different Mole Ratios

No	Observed wavenumber (cm^{-1})				Reported value (cm^{-1})	Remark
	Fe_3O_4-ZnO-0.5CuO	Fe_3O_4-ZnO-1CuO	Fe_3O_4-ZnO-2.5CuO	Fe_3O_4-ZnO-5CuO		
1	3443	3447	3439	3435	3447*	O-H stretching vibration
2	875	839	839	830	850**	Cu-O stretching
3	612	620	615	618	610*	Zn-O stretching
4	580	570	527	591	585*	Fe-O stretching vibration
6	490	406	422,415 403	484,456 406	400-500***	Cu-O and Zn-O stretching

* Kulkarni *et al*., 2017 ** Muhamad *et al*., 2007 *** Vanaja *et al*.,2016

Characterization by SEM-EDS

SEM is a scanning electron microscope that illustrates the sample surface by scanning with a beam of high-energy electrons. X-ray in the SEM can be used to identify the elemental composition of a sample by a technique known as energy dispersive x-ray (EDS). (Abd Mutalib *et al*., 2017). Figure 4 shows the SEM images of the nanocomposites. The surface morphology of Fe_3O_4- ZnO- 0.5CuO nanocomposite was found to have quasi spherical shape particles. When the mole ratio of CuO increased both spherical and clew like shape particles were also observed in Fe_3O_4-ZnO - 1CuO, Fe_3O_4- ZnO- 2.5 CuO and Fe_3O_4-ZnO- 5 CuO nanocomposites.

Figure 5 depicts EDS spectra of nanocomposites with different mole ratios. The peaks corresponding to Fe, Zn, Cu and O confirmed the formation of Fe_3O_4- ZnO- CuO nanocomposites. Three peaks each for Fe, Zn and Cu were observed. A peak less than 1 keV is O peak. Table 5 shows the weight percents of elements found in Fe_3O_4-ZnO-CuO nanocomposites with different mole ratios. It was found that as mole of CuO was increased from the weight of Cu also increased. Some impurity peaks were observed. Among them Fe_3O_4-ZnO- 5CuO was found to have the lowest impurity.

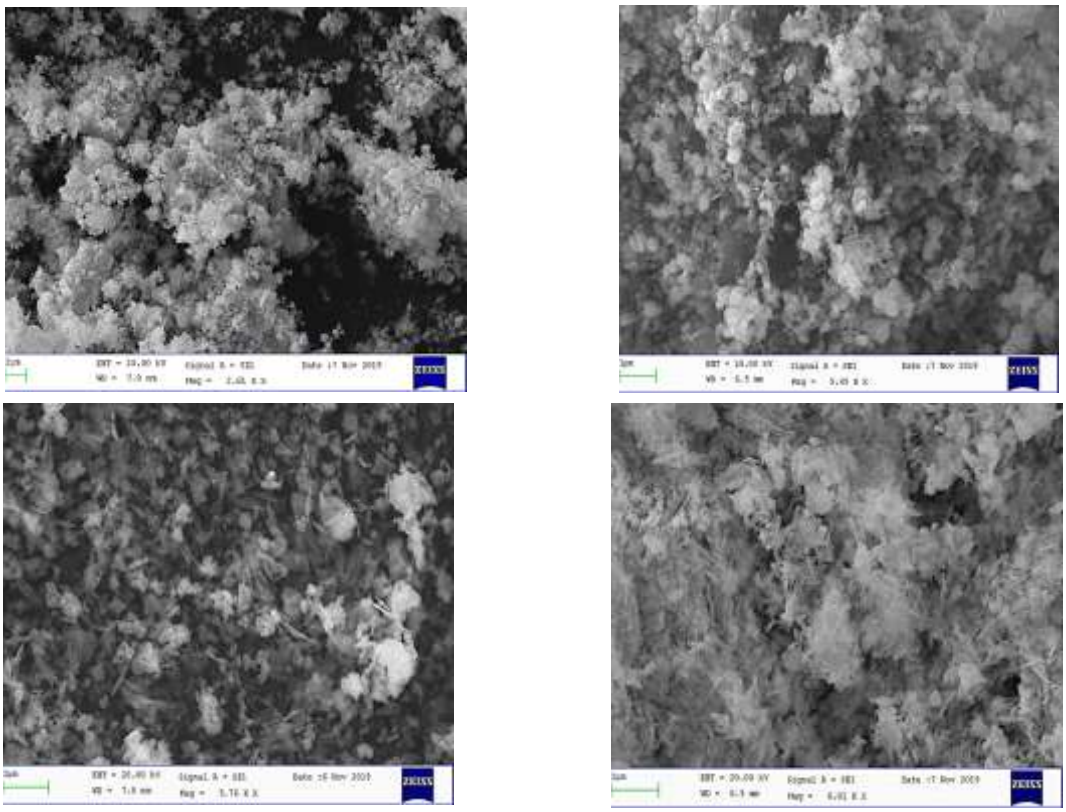

Figure 4 SEM images of (a) Fe_3O_4-ZnO-0.5CuO (b) Fe_3O_4-ZnO-CuO (c) Fe_3O_4-ZnO-2.5CuO (d) Fe_3O_4-ZnO-5CuO nanocomposites

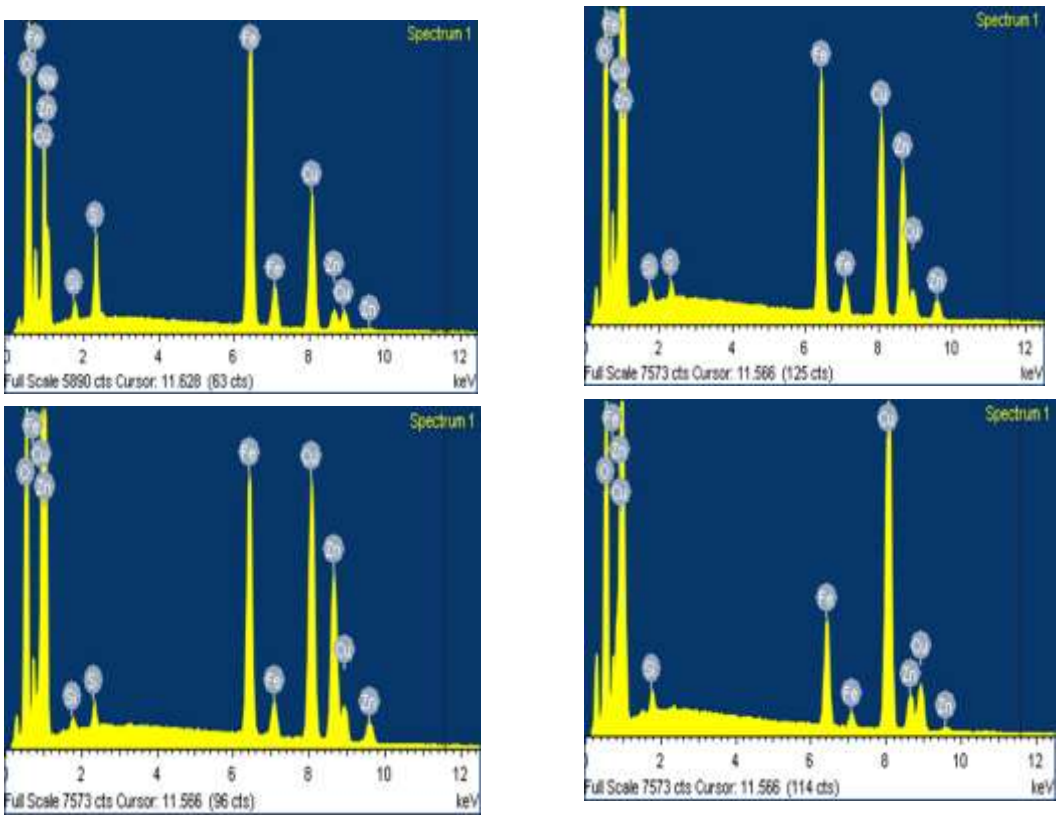

Figure 5 EDS images of (a) Fe_3O_4-ZnO-0.5CuO (b) Fe_3O_4-ZnO-CuO (c) Fe_3O_4-ZnO-2.5CuO (d) Fe_3O_4-ZnO-5CuO nanocomposites

Table 5 Weight Percent of Fe_3O_4-ZnO-CuO Nanocomposites with Different Mole Ratios

No	Sample	Weight Percent (%)						
		Fe	Cu	Zn	O	Na	S	Si
1	Fe_3O_4-ZnO-0.5CuO	15.94	27.79	24.72	27.85	1.27	1.78	0.65
2	Fe_3O_4-ZnO-1 CuO	15.89	28.31	27.44	27.46	-	0.46	0.44
3	Fe_3O_4-ZnO-2.5CuO	15.79	33.18	26.96	23022	-	0.55	0.30
4	Fe_3O_4-ZnO-5CuO	15.73	38.16	23.34	22.52	-	-	0.25

Characterization by TEM

Figure 6 is the TEM image of Fe_3O_4 -ZnO - CuO nanocomposite. TEM image of the magnetic Fe_3O_4-ZnO-CuO nanocomposite shows the cubic morphology and the crystallite size obtained by TEM was not much different from the data obtained by XRD.

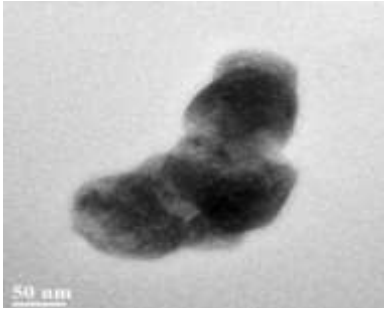

Figure 6 TEM image of Fe_3O_4-ZnO-CuO nanocomposites

Thermal Analysis by TG-DTA

Figure 7 shows the TG-DAT thermograms of Fe_3O_4-ZnO- CuO nanocomposites with different mole ratios. In all the thermograms, small endothermic peaks were observed due to removal of physically sorbed water. In the heating temperature range of 40˚C to 600˚C, small weight losses of less than 7% were observed in all nanocomposites indicating the thermal stability of the prepared nanocomposites. In Fe_3O_4-ZnO- 5CuO the smallest weight loss of 3% was observed compared to other nanocomposites with different mole ratios Table 6.

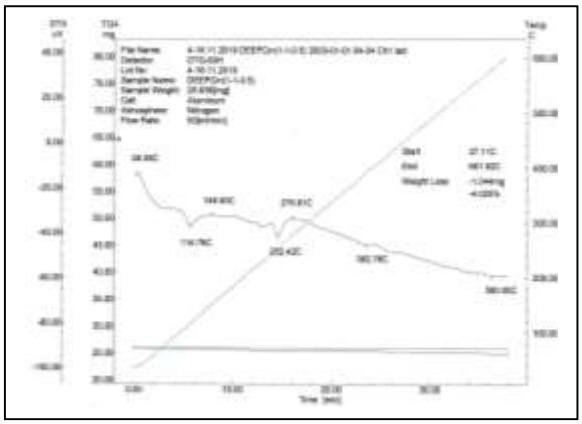

(a)

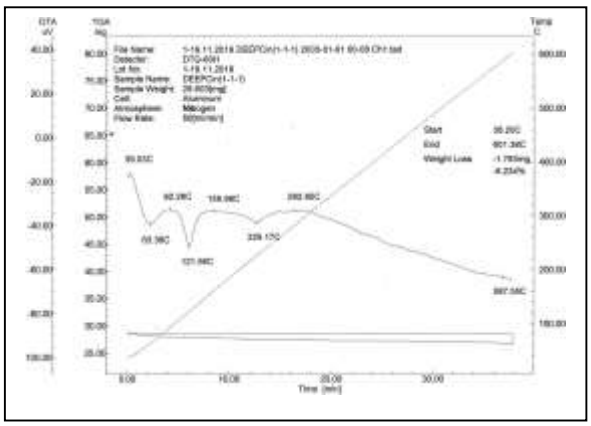

(b)

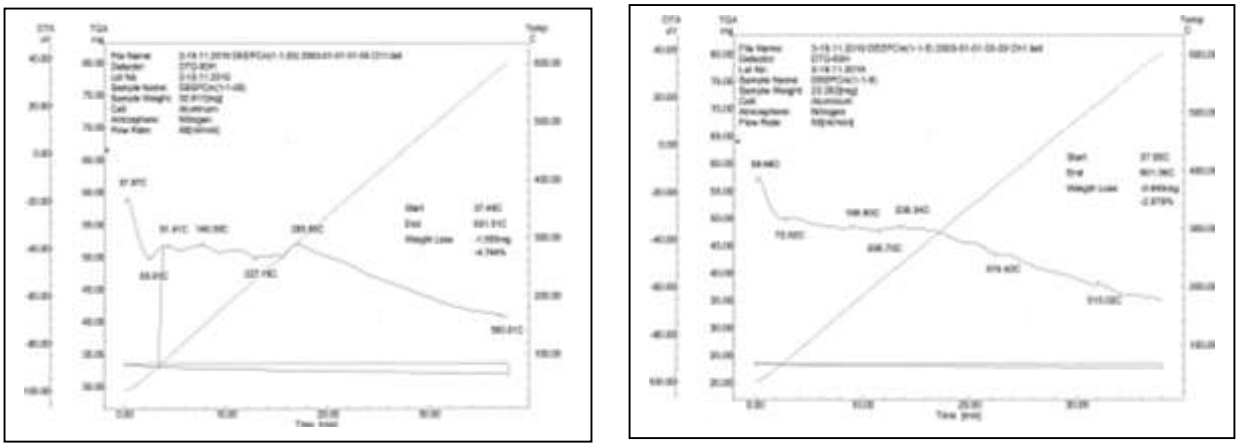

(c) (d)

Figure 7 TG-DTA Thermograms of (a) Fe_3O_4- ZnO- 0.5CuO (b) Fe_3O_4- ZnO- CuO (c) Fe_3O_4- ZnO- 2.5CuO (d) Fe_3O_4-ZnO-5CuO nanocomposites

Table 6 Weight Loss Percent of Fe_3O_4-ZnO-CuO Nanocomposites with Different Mole Ratios

No	Samples	Weight loss (%)
1	Fe_3O_4-ZnO-0.5CuO	4.025
2	Fe_3O_4-ZnO- 1CuO	6.234
3	Fe_3O_4-ZnO-2.5 CuO	4.764
4	Fe_3O_4-ZnO-5 CuO	2.979

Magnetic Property of Fe_3O_4-ZnO-CuO Nanocomposites

Figure 8 depicts a visual confirmation of the magnetic activity of Fe_3O_4-ZnO-5CuO nanocomposite. The heterogeneous nanocomposites suspended in solution were attracted towards a magnet. This showed that the Fe_3O_4-ZnO-5CuO nanocomposite used as a photocatalyst can be separated out from the suspension using a magnet on completion of the reaction suggesting its potential use in large scale water treatment.

Figure 8 magnetic properties of prepared Fe_3O_4-ZnO-5CuO nanocomposites

Conclusion

Magnetic Fe_3O_4- ZnO- CuO nanocomposites with different mole ratios have been prepared using sol-gel method. X-ray diffraction analysis showed the cubic structure of composites and the crystallite sizes of 34.1 nm, 23.4 nm, 25.1 nm and 23.2 nm were observed for Fe_3O_4-ZnO- CuO nanocomposites with different mole ratios. FT IR spectra revealed the presence of the characteristic

peaks of Fe-O, Zn-O and Cu-O in the nanocomposites. Spherical and clew like shape particles were observed in Fe_3O_4-ZnO-5CuO nanocomposites by SEM images. EDS showed the presence of Fe, Zn, Cu and O atoms. Among them Fe_3O_4- ZnO- 5CuO nanocomposites showed having lowest impurity. TEM image of Fe_3O_4-ZnO- CuO nanocomposites showed the cubic morphology. According to TG-DTA thermograms, small weight losses of less than 7 % were observed in all nanocomposites indicating the thermal stability of the nanocomposites. Magnetic property of the photocatalyst Fe_3O_4-ZnO-CuO nanocomposites can improve the reusability of the for water treatment.

Acknowledgements

The authors would like to thank to Dr Cho Cho Than, Professor and Head, Department of Chemistry, Taunggoke Degree College, for her provision of the research facilities. We also would like to express our profound gratitude to Myanmar Academy of Arts and Science for allowing to present this paper.

References

Abd Mutalib, M., Rahman, M.A., Othman, M.H.D., Ismail, A.F and Jaafar, J. (2007)."M*embrane Characterization*", vol.5 (3), pp.161-179

Akir, S., Barrs, A., Coffinier, Y., Bououdina, M., Boukherroub, R. and Dakhlaoui-Omrani, A. (2016). "Eco-friendly Synthesis of ZnO Nanoparticles with Different Morphologies and their Visible Light Photocatalytic Performance for the Degradation of Rhodamine B", *Ceram. Int*. vol. 42(8), pp. 10259-10265

Heravi, M.M., Beheshtiha S.Y.S., Dehghani, M. and Hosseintash, N. (2015). "Using Magnetic Nanoparticles Fe_3O_4 as a Reusable Catalyst for the Synthesis of Pyran and Pyridine Derivatives via One-pot Multicomponent Reaction", *Journal of the Iranian Chemical .Society*, vol.2(11), pp. 2075-2081

Hou, X., Wang, L., Li, F., He, G. and Li, L. (2016). "Controlled Loading of Gold Nanoparticles on ZnO Nanorods and their High Photocatalytic Activity. *Mater.Lett.*, vol. 159, pp.502-505

Kulkarni,S.D., Kumbar, S. M., Menon, S. G., Choudhari, K. S. and Santhosh. C. (2017). "Novel Magnetically Separable Fe_3 O_4 @ZnO Core–Shell Nanocomposite for UV and Visible Light Photocatalysis". *Advanced Science Letters*, vol. 23, pp.1724–1729

Magneshwari, K., Nataraj, D., Pal, T., Sathyamoorthy, R.and J. Park, J. (2015)." Improved Photocatalytic Acitivity of ZnO Coupled CuO Nanocomposites Synthesized by Reflux Condensation Method". *J. Alloys Compd*, vol.625, pp. 362-370

Muhamad, E.N., Irmawati, R. and Abdullah. A.H. (2007). "Effect of Number of Washing on the Characteristics of Copper Oxide Nanopowders". *The Malaysian Journal of Analytical Sciences*, vol.11, pp. 294-301

Taufik, A., Kalim,I. and R. Saleh.(2015)."Preparation, Characterization and Photocatalytic Activity of Multifunctional Fe3O4/ZnO/CuO Hybrid Nanoparticles".*Materials Science Forum*, vol.827, 37-42

Taufik, A. and Saleh. R. (2017). "Adsorption and Sonocatalytic Performance of Magnetite ZnO/CuO with NGP Variation". *Ceramics International*, vol.43, pp. 3510-3520

Vanaja, A. and Rao. K. S. (2016). "Precursors and Medium Effect on Zinc Oxide Nanoparticles Synthesized by Sol-Gel Process". *International Journal of Applied and Natural Sciences,* vol .5(1), pp. 53-62

Xuan, S., Jiang, W., Gong, X., Hu, Y. and Chen, Z. (2008). "Magnetically Separable Fe_3O_4 / TiO_2 Hollow Spheres: Fabrication and Photocatalytic Activity". *The Journal of Physical Chemistry C*, vol.113 (2), pp.553-558